

Design and Initial Operation of a Small Low-cost Hall Thruster

IEPC-2017-534

*Presented at the 35th International Electric Propulsion Conference
Georgia Institute of Technology • Atlanta, Georgia • USA
October 8 – 12, 2017*

Matthew J. Baird¹, Nagual A. Simmons² and Dr. Kristina M. Lemmer³

Western Michigan University, Kalamazoo, MI, 49008, USA

Abstract: A 200 W Hall Effect Thruster (HET) was designed at the Aerospace Laboratory for Plasma Experiments (ALPE) at Western Michigan University (WMU) with the motivation to design and build a low-cost HET that could be operated at lower power and low flow rate for testing at smaller vacuum facilities. Preliminary designs were based on the theory behind electric propulsion and plasma physics. The initial design of the Western Hall Thruster was modeled with COMSOL Multiphysics® simulation software to refine the magnetic circuit and analyze the gas flow through the anode. Fabrication was completed at WMU, and the magnetic field was tested at ALPE and NASA Glenn Research Center. Initial thruster operation was performed at ALPE. Two stable operating points, 130 W and 200 W, were used to characterize the performance of the thruster and were compared to anticipated values.

Nomenclature

e	=	electron charge
L	=	channel length
\dot{m}_a	=	anode mass flow
\dot{m}_c	=	cathode mass flow
\dot{m}_p	=	total propellant flow
m_i	=	ion mass
P_k	=	keeper power
P_d	=	discharge power
P_{mag}	=	magnet power
P_T	=	total power
r_i	=	ion radius
r_L	=	Larmor radius
T	=	Thrust
v_I	=	ion velocity
V_b	=	beam voltage
η_c	=	cathode efficiency
η_o	=	electrical efficiency
η_T	=	total efficiency

¹ Graduate Student Research Assistant, Mechanical and Aerospace Engineering, matthew.j.baird@wmich.edu.

² Graduate Student Research Assistant, Mechanical and Aerospace Engineering, nagual.a.simmons@wmich.edu.

³ Assistant Professor, Mechanical and Aerospace Engineering, kristina.lemmer@wmich.edu.

I. Introduction

The ability to show that an accessible Hall effect thruster (HET) can be designed, built, and tested by universities with minimum resources would be attractive to the aerospace community. HETs can be designed for many applications ranging from satellite orbit correction to deep space missions and will play an exciting role in the future of space travel. NASA has specifically tasked HETs for use in future missions in the Technology Roadmap ¹. The goal of this work was to design and prototype a small HET that is accessible to any university with standard high vacuum, electrical, and machining resources. This HET is a low-cost alternative that provides significant educational value to students working on the project. By opening this field of study to more researchers and encouraging more universities to become involved in EP research, more knowledge will be contributed to the understanding of HETs. This increased understanding will contribute to better HET designs and more widespread use of HETs for space propulsion.

The thruster presented in this paper, the 44-mm Western Hall Effect (WHT-44), was designed, simulated, and tested at Western Michigan University's Aerospace Laboratory for Plasma Experiments (ALPE). The layout of this report is as follows: first the design of the WHT-44 is discussed. This includes the scaling laws and practices that were used; second, we talk about simulation and mapping of the magnetic field; lastly, we discuss the telemetry that was gathered under initial operation.

II. Design

HETs have relatively simple geometry compared to other electric propulsion thrusters, placing them within the manufacturing capability of most universities. This design focuses on the main characteristics of an HET: channel dimensions, magnetic circuit, and anode. Successful design and operation of this HET promotes ongoing measurements and testing to be performed at ALPE. Detailing the design and fabrication process serves as an example for universities with limited resources to replicate and improve upon the thruster while performing meaningful research on their own HET.

A. Dimensional Iteration and Simulation of the Magnetic Lens

Many iterations of the design were conceived. This process began with the assumption that the thruster would achieve a target discharge power of 250 W and be capable of being operated within the ALPE testing facility. Mathcad was used to generate theoretical parameters such as required magnetic field, channel outer radius, width, thrust, propellant flowrate, etc. The basic dimensions were placed into COMSOL Multiphysics® followed by population of coil, anode, and shielding details. Many iterations were not accepted simply because the dimensions could not contain a center coil sufficiently large to support the required magnetic field, or a near zero magnetic field could not be achieved at the anode. Another common reason for a rejected iteration was magnetic saturation. Saturation profiles were used when calculating the magnetic field throughout the thruster, and, in some cases, the applied magnetic field by the coils could not be supported by smaller diameter cores. To prevent the issue of magnetic saturation, core diameters were increased to operate at the knee of the magnetic hysteresis linear region. This was repeated until all dimensional and magnetic requirements were met.

The magnetic lens design has direct implications on lifetime and performance of HETs. An ideal magnetic lens is designed in such a way that magnetic field is strongest near the exit plane and quickly approaches zero just before the anode surface^{2,3}. The curvature of the magnetic field lines may also be designed to decrease ion bombardment with the channel walls and increase thruster life in what has been termed magnetically shielded (MS) HETs⁴. MS HETs require complex magnetic circuit designs that are outside the scope of the WHT-44.

The magnetic lens is created with a magnetic circuit that consists of several outer coils and one center coil. Initial simulations resulted in the WHT-44 having six outer electromagnetic coils to provide the thruster with a consistent magnetic field at the exit plane. The cores are held to the thruster front plate by direct threading, and they are secured to the back thruster pole with a nut. As a result, no material was removed from the core, and the magnetic resistance was minimized to the thread interfaces, producing a strong magnetic field at the exit plane. Shielding is required to reduce the magnetic field at the anode. Internal trim coils could also be used to reduce the magnetic field strength at the anode by running the current in opposition with respect to the current in the main magnetic coils. While trim coils were considered, they would have greatly increased the complexity of the thruster, and shielding was sufficient to modify the magnetic lens.

The core material and shielding have non-linear magnetic saturation limits that require special consideration. The B-H curves were used to determine when magnetic saturation would occur at a given applied magnetic field. The iron (core material) and MuMetal® (shielding material) magnetically saturate around 1.6 and 0.6 Tesla, respectively. The effects of various shielding thicknesses and widths were simulated using COMSOL Multiphysics® and the dimensions

chosen provide a balance between a strong exit plane magnetic field and the desired magnetic field shape along the channel.

Due to a constant packing factor, the number of turns on each coil did not have a notable impact on the results of the magnetic lens. If a smaller diameter wire was used, the number of turns increased by the same factor that the wire's current capacity decreased, resulting in the same overall coil current density. For ease of fabrication, high temperature 22-gauge double insulated magnet wire was chosen to reduce the number of turns needed to exactly 300. The current ratio between outer and inner coils was also investigated, yielding the ideal inner to outer current ratio of 1.

B. Anode Design

The anode was designed to provide even gas distribution and, thus, discharge within a channel. Two methods for analyzing gas flows are the continuum approach and rarefied flow modeling. The continuum approach treats the fluid as a whole and disregards intermolecular interactions. Rarefied flow modeling is the study of gas flow at near vacuum and takes molecular interactions into account. Typically, a rarefied flow model would be used to determine the flow from the anode to a vacuum; however due to the scope, required knowledge and computational power involved with performing a rarefied study, the continuum approach was used as an approximation for the WHT-44 anode design. Flow simulation of the WHT-44 anode design was performed in ANSYS®. From the ANSYS® simulations, it is clear that from a continuum perspective, the gas is evenly distributed within the channel between 2 and 5 mm from the anode plate.

C. Thermal Considerations

Due to the temperature increase of all thruster components, thermal expansion of the components was accounted for when designing the thruster. For these calculations, a temperature rise of 300 K was assumed. Thermal expansion coefficients were determined using material properties obtained from an online database. With the expected expansion of each component calculated, the next step was to find the areas where expansion could cause damage. Worst case scenarios were used by assuming that only one part would expand at a time and checking for interference. The areas of most concern were where the anode and center core contact the boron nitride (BN). Once the dimension changes were identified, the model was updated.

D. Fabrication

All major components were machined at WMU on provided lathes and mills. No special equipment was needed; only tooling had to be purchased to drill exceptionally small holes, machine tough material, and ream holes for tight tolerances. Most components were cleaned in an ultrasonic bath and dried just before final assembly. The BN channel and coils were not cleaned using this method, and great care was taken during the machining process to prevent oil and dust contamination.

The magnets were wound on an aluminum rod, which was cut to a diameter 127 μm greater than the core diameters. This allowed the magnets to fit snugly over the cores while making them easy to install and remove. After winding, the coil was slipped off the aluminum rod; however, a small amount of shielding had been removed from the inner windings while removing the coils from the aluminum rod. There is room to improve this process to prevent coil damage.

The anode is made up of four parts: the front plate with twenty 0.76-mm-diameter holes, the channel with two 1.59 mm gas tube holes, and two gas tubes. All anode components were machined from 316 stainless steel. The anode front plate and anode channel were spot welded together, at the inside lip, at 6 points. The gas tubes were brazed onto the channel part. Although the brazing alloy contains 28% zinc, it is used in very small amounts and should not be problematic for use in a vacuum chamber.

The gas feed was made up of several Swagelok components. Beginning with the vacuum chamber feedthrough the feed system consists of flexible tubing, a dielectric break, a straight tube section with an electrical connection for the anode, and a tube adapter. The gas was then split into two gas tubes using a T-joint and two 90° elbow Swagelok fittings before it was connected to the gas tubes that had been brazed onto the anode.

E. Hardware and Assembly

Kapton and fiber glass tape were used liberally to prevent the magnets shorting to the pole pieces and to insulate exposed discharge voltage potentials behind the thruster. 304 stainless steel fasteners and Bellville washers were used to increase BN compliance. Finally, the anode was held in place by twin gas tubes with stainless steel push nuts and ceramic washers.

F. Completed Thruster Specifications

The final channel outer diameter was selected to be 44 mm with a channel width of 5 mm. Applying scaling laws from Gobel and Katz for an optimized HET allows the estimation of an anode mass flow rate of 0.96 mg/s of xenon and a discharge current of 0.87 A.²

The COMSOL Multiphysics® simulation shows the WHT-44 yields a maximum radial magnetic fields strength of 460 G. Figure 1 represents the magnetic field varying axially in the channel for both simulated (COMSOL Multiphysics®) and measured values. After simulation, the magnetic field strength profile along the WHT-44 channel was used to approximate the ionization region of the thruster, which can be determined from where the Hall current is unsustainable due to the larger Larmor radius at the lower magnetic field strength. Retaining the assumption of an electron temperature of 40 eV inside the channel and setting the Larmor radius of an electron to 2.5 mm, we see that a magnetic field strength greater than 93 G will support electron mobility. This results in an ionization region length, L , of about 7 mm. Consulting our previous conservative ion Larmor radius (476 mm) and electron Larmor radius (2.5 mm) values, it is shown that the designed 13 mm channel length satisfies the Larmor radius requirements. Using Eq. (1) and Eq. (2), the ion exit velocity and thrust are estimated and yield 18.5 km/s and 17.8 mN, respectively. Discharge power is approximated by multiplying the discharge area by our estimated current density of 0.1 to 0.15 A/cm². Therefore, the WHT-44 power ranges from 144-216 W. The coil resistance is calculated using a resistivity at an exaggerated temperature of 600 K to yield a total coil power consumption of 0.53 W. Plugging these values into Eq. (3) yields an electrical utilization efficiency of 0.998. The cathode mass flow rate will be an estimated 0.3 mg/s. From Eq. (4) the cathode efficiency is roughly 0.762. Lastly, supplying these efficiencies into Eq. (5), yields an overall maximum efficiency of 0.51.

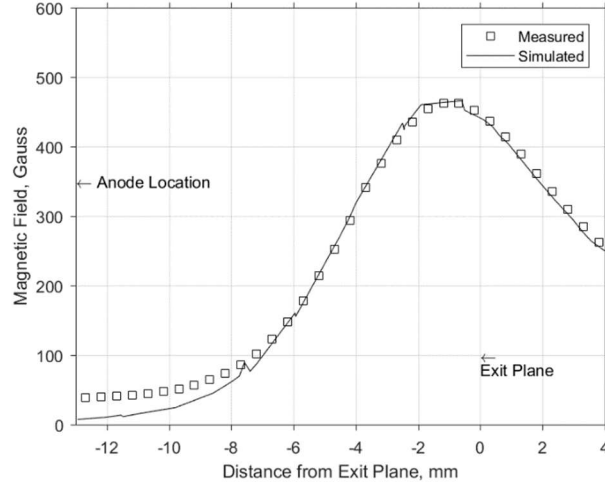


Figure 1. Magnetic field strength varying radially in channel. Comparison of the simulated and measured magnetic field strength varying radially down the WHT-44 channel.

$$v_i = \left(\frac{2eV_b}{m_i} \right)^{\frac{1}{2}} \quad \text{Eq. (1)}$$

$$T = \dot{m}_a v_i \quad \text{Eq. (2)}$$

$$\eta_o = \frac{P_d}{P_T} = \frac{P_d}{P_k + P_d + P_{mag}} \quad \text{Eq. (3)}$$

$$\eta_c = \frac{\dot{m}_a}{\dot{m}_p} = \frac{\dot{m}_a}{\dot{m}_a + \dot{m}_c} \quad \text{Eq. (4)}$$

$$\eta_T = \frac{1}{2} \frac{T^2}{\dot{m}_a P_d} \eta_o \eta_c \quad \text{Eq. (5)}$$

III. Initial Testing and Operation

After fabrication of the WHT-44, far field magnetic map testing was performed at NASA Glenn Research Center (GRC). Additional magnetic field measurements and initial startup occurred at ALPE. Results of the magnetics were compared to COMSOL Multiphysics® simulations and estimated thruster operating parameters were compared to observed values at the nominal operating condition.

G. Magnetic Field Testing

A VI was written in LabVIEW to automatically map and log the magnetic field strength axially along the WHT-44 channel. The Gauss meter used was a Lakeshore Cryotronics Model 425 with a 457 mm aluminum stem probe. Magnetic field strength was measured at 0.5 mm steps from 4.18 mm above the anode surface to 40 mm beyond the exit plane. The probe could not measure closer than 4.18 mm to the anode surface due to the sensor location inside the probe. These data were exported to excel and compared to the simulated data shown previously in Figure 1.

Magnetic mapping equipment at GRC was used to establish the magnetic field topography outside of the thruster in a 270 mm x 270 mm plane directly forward of the thruster. The plane was level with the center line of the thruster and three-dimensional magnetic field measurements were taken with 1 mm resolution. The resulting data were used to create magnetic field streamline plots shown in Figure 2. The magnetic map shows the separatrix; electron mobility is increased if the cathode is placed inside⁵.

H. Facility and Setup

The test facility is Western Michigan University's ALPE. ALPE's vacuum chamber uses a single CTI-250 Cryogenic Pump paired with a CTI 8510 Compressor with pumping capacity of roughly 2,000 l/s nitrogen and an Edwards 80 E2M80 roughing pump that has a capacity of 25 l/s. The vacuum chamber is 1-m-diameter and 1.5-m-long. Chamber pressure is measured by cold cathode and thermocouple gages. This facility is capable of a base pressure around 1E-7 torr. Data collection was performed using a National Instruments USB-6356 DAQ X. To verify the health of the thruster the discharge current was observed through a 100MHz Tektronix oscilloscope with a 1-volt to 1-amp Pearson coil. Two Alicat mass flow controllers rated for 0-10 (cathode) and 0-100 (anode) scfm were used to control the Xenon flow. A heaterless 1.6-mm hollow cathode from Plasma Controls, LLC was used to start and operate the WHT-44. The cathode was configured such that it's maximum current capability was approximately 1.5 A.

Two Sorensen power supplies, the DLM600-6.6 and DCS300-3.3, were used to operate the anode and keeper respectively. The electromagnets were controlled with a Lambda Gen100-15 power supply. The cathode and thruster body are electrically floating. The anode, keeper, and magnets are tied to cathode common. Figure 3 shows the cathode and thruster positions in the chamber.

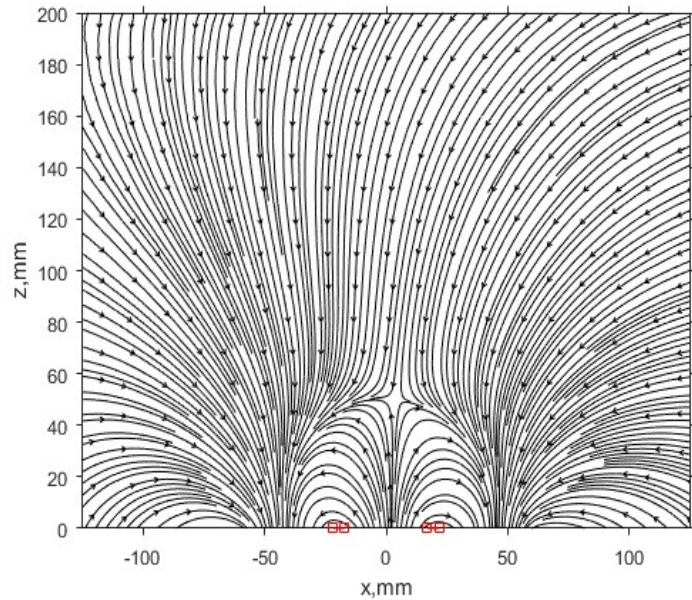


Figure 2. Far field magnetic Field Map. Magnetic field topology of the WHT-44 with one amp being delivered to the coils. The thruster channel is depicted by the squares.

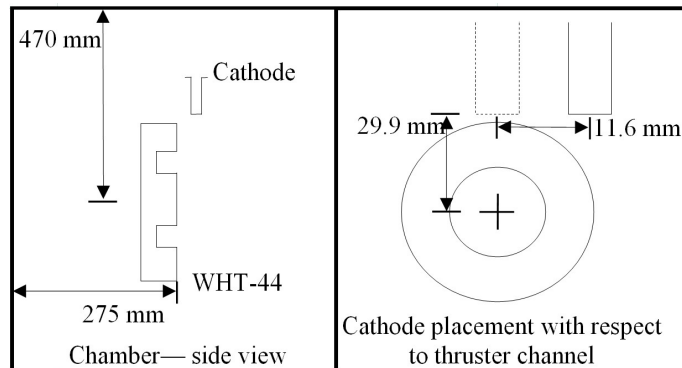


Figure 3. Cathode and thruster placement. (Left) Shows the side view placement of the thruster with respect to the chamber walls. (Right) Shows the placement of the cathode with respect to the thruster channel.

I. Startup Procedure, Stable Operation, and Test Points

After difficulty performing a normal thruster startup or performing a glow mode startup, the thruster was successfully started by “burp” starting of the cathode with both inner and outer magnets on, thruster gas flowing, and discharge energized. Burp starting of the cathode involved shutting off the mass flow controller outlet isolation valve for a set duration such that a known volume of xenon could build up, then opening the isolation valve. To allow a fixed volume of gas through the cathode. This process simultaneously started the cathode and thruster.

Safe operation was defined as a satisfactory view port window inspection that yielded no arcing, hotspots, or visible discharge fluctuations, no excessive temperature rises, and stable cathode keeper voltage and current. Two such conditions at a discharge voltage of 200V were found. The current density at these points was a reasonable discharge current density of 107-mA/cm² and a slightly elevated current density of 170-mA/cm². The first thrust point was a 130 W condition with a discharge voltage of 200V. The second thrust point was a 200 W condition with a discharge voltage of 200 V. Table 1 contains a summary of all operating parameters for these two conditions.

While operating the thruster a Pearson coil current monitor and oscilloscope was used to monitor the discharge current. The thruster discharge current was observed as a function of time for both operating points. The discharge current was very oscillatory. The peak-to-peak current and oscillatory behavior increased from the 130 W to 200 W testing point. Figure 4 shows the oscillatory behavior of the discharge current at the 130 W operating point. The peak-to-peak amplitude varies from 2 to 3.5 amps around 38 kHz. At the higher, 200 W, test point the frequency ranged from 20-60kHz with a peak-to-peak amplitude between 3-7 A.

IV. Post-experiment Examination

The thruster ran for a total of 15 hours during the initial testing. Afterwards, the WHT-44 was removed from the vacuum facility and examined. Cracking of the channel, shown in Figure 5, where the top pole sits on the ceramic seat, was noticeable.⁶ Spalling was also observed on the anode surface.

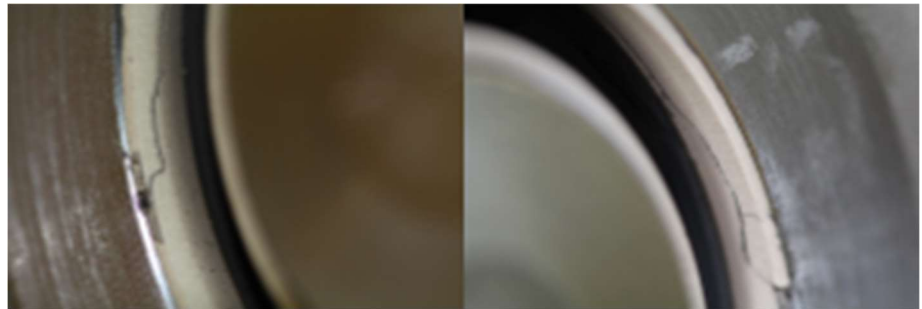


Figure 5. Cracking in ceramic channel near the top pole. The ceramic channel had noticeable cracking after 15 hours of operation where the top pole came in contact with the ceramic channel.

Table 1. Thruster Operating Parameters

Summarizes the thruster and cathode operating conditions for both the 130 W and 200 W test point conditions.

Parameter	130W Thrust Point	200W Thrust Point
Cathode Keeper Parameters	11V/0.3A (6 sccm)	10V/0.2A (1 sccm)
Discharge Parameters	200V/0.66A (6 sccm)	200V/1.04A (9 sccm)
Magnet Current	0.30A	0.25A
Facility Pressure	7E-4 Torr	5.6E-4 Torr
Electrical Status	Body Floating	Body Floating

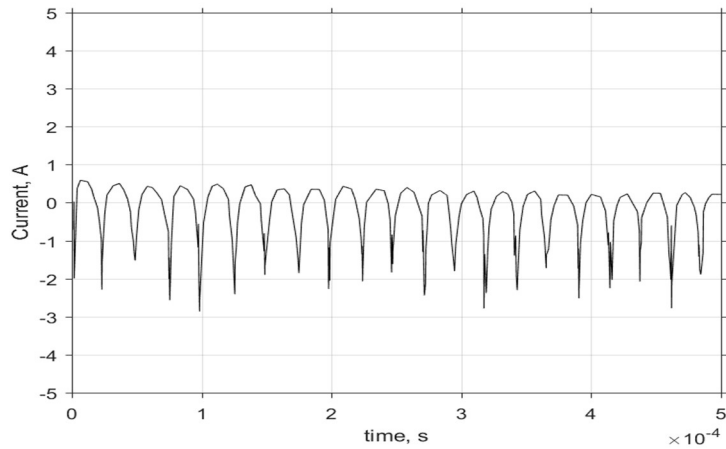


Figure 4. Hall thruster current oscillations. Discharge current oscillation observed at the 130 W operation point.

V. Conclusion

It has been shown that a university with minimal machining and vacuum chamber facilities can successfully design and operate a low-cost HET for experimental use. Machining tolerances need to include thermal expansion. The magnetic field mapping, both near and far field, were as expected. The far field magnetic map identified the separatrix. The high current oscillations observed in the thruster could be a combination of poor coupling of the cathode with the thruster and a non-optimized anode design. Since the WHT-44 was not able to start normally or using glow discharge the latter is believed to be the dominate cause of the high discharge current oscillations.

Acknowledgments

The Arthurs would like to thank Western Michigan University's office of the Vice presidents for awarding us with the undergraduate research excellence award. With this money the purchase of all the materials needed for fabrication were made.

References

- ¹NA, "TA 2: In-Space Propulsion Technologies. 2015". NASA Technology Roadmaps, 2015.
- ²Goebel DM, Katz I. *Fundamentals of Electric Propulsion: Ion and Hall Thrusters*, Wiley, 2008, Chaps. 2,3, and 7.
- ³Hofer RR., "Development and Characterization of High-Efficiency, High-Specific Impulse Xenon Hall Thrusters," Ph.D. Dissertation, Aerospace Dept., University of Michigan, Ann Arbor, MI, 2004.
- ⁴Mikellides, I.G., Katz, I., Hofer, R.R., "Design of a Laboratory Hall Thruster with Magnetically Shielded Channel Walls, Phase I: Numerical Simulations," *47th Joint Propulsion Conference and Exhibit*, July 31st – August 3, 2011, San Diego, California.
- ⁵Sommerville, J.D., King, L.B., "Hall-Effect Thruster – Cathode Coupling Part I: Efficiency Improvements from an Extended Outer Pole," *Journal of Propulsion and Power*, Vol. 27, No. 4, July-August 2011.
- ⁶Baird M, Thompson J, Simmons N., "Design of a Hall Effect Thruster," Senior design Project, Mechanical and Aerospace Engineering Dept., Western Michigan University, Kalamazoo, MI, 2016.